European Review for Medical and Pharmacological Sciences 2020; 24: 1420-1427

MicroRNA-34a suppresses neuronal apoptosis and alleviates microglia inflammation by negatively targeting the Notch pathway in spinal cord injury

Y.-P. JIAN[1], S.-J. DONG[2], S.-S. XU[1], J. FAN[1], W.-J. LIU[1], X.-W. SHAO[1], T. LI[1], S.-H. ZHAO[1], Y.-G. WANG[1]

[1]Department of Spine Surgery, Xuchang Central Hospital, Xuchang, China
[2]Department of Clinical Testing Center, Xuchang Central Hospital, Xuchang, China

Abstract. – OBJECTIVE: The purpose of this study was to investigate role of inhibition of microRNA-34a (miR-34a) in neural damage and repair after spinal cord injury, and to explore the underlying mechanism.

MATERIALS AND METHODS: In BV2 microglia, we conducted classical activation using lipopolysaccharide (LPS) and pre-treatment using miR-34a mimics. The expressions of miR-34a, Notch 1, and Jagged 1 were detected by quantitative Real Time-Polymerase Chain Reaction (qRT-PCR). Moreover, the protein expressions of inflammatory microglia markers were evaluated by Western blotting. *In vivo*, SCI model was successfully established in rats. Subsequently, the expression levels of miR-34a, Notch 1, and Jagged 1 levels within 1 week were measured by qRT-PCR. Meanwhile, protein expressions of inflammatory mediators were determined by enzyme-linked immunosorbent assay (ELISA) assay. Immunofluorescence was conducted to display the activation degree of microglia and residual neural structure. Furthermore, locomotor function recovery was estimated using BBB rating scale.

RESULTS: Compared with the only LPS-activated group, pre-treatment of miR-34a mimics significantly decreased the expressions of Notch 1 and Jagged 1. Similarly, the protein expressions of CD11b and iNOS were significantly down-regulated. *In vivo*, the levels of Notch 1 and Jagged 1 within 1 week increased significantly, while miR-34a was negatively regulated following spinal cord injury (SCI). Furthermore, the contents of interleukin-1 beta (IL-1β) and IL-6 were reduced with the treatment of miR-34a mimics when compared with SCI group. With the treatment of miR-34a, the number of inflammatory microglia decreased significantly, and the remaining neural structure was similarly improved. In addition, locomotor function recovery of hindlimbs in rats was significantly ameliorated after the administration of miR-34a mimics.

CONCLUSIONS: Increase of miR-34a suppresses neuronal apoptosis and alleviates microglia inflammation by negatively targeting the Notch pathway, thereby improving neural recovery and locomotor function.

Key Words:
Spinal cord injury (SCI), MiR-34a inhibition, Notch pathway, Inflammation.

Introduction

Spinal cord injury (SCI) is a traumatic disease of the central nervous system (CNS), with high incidence, disability, and mortality[1,2]. After a primary injury caused by fracture and compression, a series of pathophysiological alterations further aggravate SCI, including secondary inflammatory reaction, tissue hypoxia, neuronal necrosis and apoptosis, as well as local inhibitory microenvironment[3]. This may eventually lead to severe sensory and locomotor dysfunction. Inflammatory response after SCI is mainly regulated by cytokines, chemokines, reactive oxygen species, as well as second messengers secreted by CNS-activated glial cells and peripheral immune cells[2,4-6]. It is the result of combined action of immune, biochemical, and pathophysiological processes. The severity of SCI depends on the mechanism of primary injury and the pathological process of secondary injury[7,8]. Therefore, it is of great significance to explore the pathophysiological changes after SCI for the research and repair of SCI.

MicroRNAs (miRNAs) are single-stranded, non-coding RNAs with 20-24 nucleotides in length. They can regulate protein expression at the epigenetic level[9-11]. MiRNAs are initially

Corresponding Author: Yigong Wang, BM; e-mail: 617693188@qq.com

transcribed from genomic DNA, mainly in the form of primary miRNA transcripts by RNA polymerase II[12,13]. The function and role of miRNAs in human diseases still need to be further elucidated. However, in recent years, several studies[14-16] have shown that miRNAs can serve as a brand-new drug target. Hu et al[17] inhibited the expression of miR-21 in neurons through miR-21 antagonists. They have found that this treatment leads to decreased recovery of hind-limb motor function, increased range of injured sites, and reduced range of normal tissues in rats. Bhalala et al[18] overexpressed miR-21 through transgene in mouse astrocytes. Their results have demonstrated that overexpression of miR-21 in astrocytes reduces hypertrophy response to SCI. Similar to miR-21, an increased expression of miR-486 was detected 7 days after SCI in the contusion model. Jee et al[19] have shown that injection of miR-486 into spinal cords of healthy mice reduces motor function and increases neuronal death. However, the exact function of miR-34a in SCI has not been fully elucidated. Currently, some researches have indicated that miR-34a plays an anti-inflammatory role in macrophage. Meanwhile, miR-34a regulates the differentiation of neural stem cells by regulating the expression of synaptic and autophagic proteins. Therefore, we speculated that miR-34a might be a potential therapy target of SCI. The aim of the current report was to explore the therapeutic effect of miR-34a on SCI and to elucidate its potential underlying mechanism.

Materials and Methods

Microglia Culture and Treatment

BV2 microglia line was obtained from Xuchang Central Hospital Laboratory. BV2 microglia were cultured in Dulbecco's Modified Eagle's Medium (DMEM; Thermo Fisher Scientific, Waltham, MA, USA) containing 10% fetal bovine serum (FBS; Gibco, Rockville, MD, USA) and 1% streptomycin and penicillin. When the density of microglia reached 90%, miR-34a mimics were transfected into microglia. Subsequently, 100 ng/mL lipopolysaccharide (LPS) was used to activate an inflammatory response in microglia. After 24 h, total RNA and protein were extracted for use.

Animals and Grouping

A total of 96 female Sprague Dawley (SD) rats were enrolled in this study to establish the SCI model. All rats were at the age of 6-8 week and weight of 200-220 g. The breeding environment was controlled at 22-25°C, with 55-65% humidity and 12 h/12 h circadian cycle. All rats were given free access to conventional food and water. Subsequently, the rats were randomly divided into three groups, including Sham group, SCI group, and miR-34a group. Rats in Sham group only received laminectomy. Rats in SCI group were injected with the same amount of normal saline intrathecally. Meanwhile, rats in miR-34a group were injected with miR-34a mimics intrathecally. This research was approved by the Animal Ethics Committee of Xuchang Central Hospital Animal Center.

Operative Procedure and Treatment

Rats were anesthetized with 10 % paraformaldehyde at a dose of 0.8 ml. After skin preparation and immobilization, back skin and muscles were cut to expose the lamina. Then, we striped the upper lamina of the spinal cord. ALLEN bump equipment (10 g × 5 cm) was used to damage spinal cord tissues. Spinal cord hemorrhage and delayed extension of hindlimbs and tail swing in rats indicated successful SCI modeling. Next, miR-34a mimics was intrathecally injected into rats of the miR-34a group. The incision was sutured and the skin was sterilized again. Auxiliary urination was conducted twice a day until the urination reflex recovered.

Western Blotting

Total protein in microglia and spinal cord tissues were extracted on ice using a total protein extraction kit containing protease inhibitors and phosphatase inhibitors. After centrifugation (13000 rpm, 10 min) at 4°C, the supernatant purified protein was obtained. The concentration of proteins was determined by double Bicinchoninic Acid (BCA) method (Pierce, Rockford, IL, USA). Subsequently, the proteins were separated by 10% sodium dodecyl sulfate-polyacrylamide gel electrophoresis (SDS-PAGE) and transferred onto polyvinylidene difluoride (PVDF) membranes (Millipore, Billerica, MA, USA) on ice. 5% non-fatty milk was prepared with Tris-Buffered Saline and Tween-20 (TBST) to block non-specific antigen for 1h at room temperature. After washing 3 times with TBST, the membranes were incubated with primary antibodies (iNOS, Abcam, Cambridge, MA, USA, Rabbit, 1:250; CD11b, Abcam, Cambridge, MA, USA, Rabbit, 1:1000; PARP-1, Abcam, Cambridge, MA, USA,

Rabbit, 1:1000; Drp-1, Abcam, Cambridge, MA, USA, Rabbit, 1:1000; glyceraldehyde 3-phosphate dehydrogenase (GAPDH), Proteintech, Rosemont, IL, USA, 1:10000) at 4°C overnight. On the next day, the membranes were incubated with corresponding secondary antibody (Goat Anti-Rabbit IgG, YiFeiXue Biotechnology, Nanjing, China, 1:3000) at room temperature for 1h. Immuno-reactive bands were visualized using enhanced chemiluminescence (ECL; Pierce, Rockford, IL, USA) on an exposure machine.

Quantitative Real Time-Polymerase Chain Reaction (qRT-PCR)

1 mL TRIzol (Invitrogen, Carlsbad, CA, USA) was added to spinal cord tissues drop-wise and homogenized after shearing. The nucleic acid-protein complex was completely separated after 5 min of incubation at room temperature. 0.5 mL TRIzol was added to microglia, followed by shanking on an ice shaker for 10 min. Subsequently, 0.2 mL chloroform was added and the tubes were violently shaken for 15 s, followed by incubation at room temperature for 3 min. The mixture was then centrifuged for 15 min at 10000 RPM and 4°C. The upper water phase was collected, and isopropyl alcohol was added. Next, the mixture was vibrated and incubated at room temperature for 10 min. After centrifugation for 10 min (10000 RPM, 4°C), RNA precipitation was collected and the supernatant was discarded. After washing RNA precipitation with 75% ethanol, the mixture was centrifuged (10000 RPM, 4°C) for 5 min. The supernatant was removed and 30 μL RNase free water was added to dissolve it. RNA concentrations were measured by NanoDrop to determine absorbances at 260 nm, 230 nm, and 280 nm, respectively. If A260/A280 was between 1.8 and 2.0, the quality of RNA was considered to be standard and could be used in subsequent experiments.

MRNA quantitative analysis was achieved using Prism 7300 Sequence Detection System (Applied Biosystems, Foster City, CA, USA). A 25 μL reaction system was prepared, including SYBR Green (12.5 μL), 10 Mm of primers (0.5 mL each from the stock), 10.5 μL of water, and 0.5 μL of the template. Specific PCR conditions were as follows: denaturation at 95°C for 10 min; 40 cycles of denaturation at 95°C for 15 s; annealing at 60°C for 30 s and extension at 72°C for 30 s. Glyceraldehyde 3-phosphate dehydrogenase (GAPDH) was used as an internal reference. Comparative threshold cycle (Ct) method, namely the $2^{-\Delta\Delta}$Ct method, was used to calculate relative expression level. Primer sequences used in this study were as follows: Notch 1, F: 5'-CGGAGGAGCTTAACTCACTTACTC-3', R: 5'-CGATAGGAAGATGTCCGAGA-3'; miR-34a, F: 5'-GCCTGTAAGCATCCATCGACTG-3', R: 5'-AGGTTGCATGTAGTGCGTCCG-3'; Jagged 1, F: 5'-ACCGCAGCATGGCATTTACAA-3', R: 5'-CGATAGATAAGCGACAATTC-3'; GAPDH: F: 5'-CGCTCTCTGCTCCTCCTGTTC-3', R: 5'-ATCCGTTGACTCCGACCTTCAC-3'.

Enzyme Linked Immunosorbent Assay

Spinal cord tissues samples were first taken from rats. An appropriate amount of phosphate-buffered saline (PBS) was added to clean the tissues. Then, the mixture was homogenized and centrifuged for 10 min to collect the supernatant. Standard product wells were set on 96-well plates, and standard products of different concentrations were successively added. Samples to be tested were added into the corresponding wells, followed by sealing with sealing films and incubation at room temperature for 30 min. Next, the liquid was discarded, and each well was filled with washing solution for 30 s (repeat for 5 times). Subsequently, enzyme standard reagent was added into each well, except blank wells. The colorant was added to each well and incubated in dark for 15 min. The termination solution was added to terminate the reaction. Absorbance (OD value) of each well at the wavelength of 450 nm was measured by zeroing in the blank hole. With the concentration of standard product as abscissa and OD value as ordinate, the standard curve was drawn to calculate the concentration of samples.

Immunofluorescence

Spinal cord tissue samples were placed in 4% paraformaldehyde for 24 h of immobilization. Subsequently, the samples were dehydrated under different concentration ethyl alcohol solutions, embedded in paraffin, and cut into 5-μm sections with a rotary microtome. After deparaffinage and antigen repair, bovine serum albumin (BSA) was utilized to block non-specific combination at room temperature for 1 h. After washing with PBS, the sections were incubated with primary antibodies (IBA-1, Abcam, Cambridge, MA, USA, Rabbit, 1:300; CD11b, Abcam, Cambridge, MA, USA, Rabbit,1:400; NF 200, Cell Signaling Technology Danvers, MA, USA, Rabbit, 1:200; caspase-3, Cell Signaling Technology Danvers, MA, USA, Rabbit, 1:400) at 4°C overnight. On

the next day, the sections were incubated with fluorescent secondary antibodies for 2 h in the dark, followed by washing again. 4',6-diamidino-2-phenylindole (DAPI) Fluoromount-G was utilized to stain the nucleus and seal the sections for 5 min. Finally, the sections were visualized using a fluorescence microscope.

Behavioral Assessment

Basso-Beattie-Bresnahan (BBB) locomotor rating scale was used to evaluate the recovery of locomotor coordination function of hind-limbs within four weeks after SCI in rats. Two blinded experimenters scored the rats on a scale of 0 to 21 as they observed their movements in an open field. The evaluation was conducted at 1, 3, 7, 14, 21, and 28 days after SCI modeling, respectively.

Statistical Analysis

Statistical Product and Service Solutions (SPSS) 16.0 (SPSS Inc., Chicago, IL, USA) statistical software was used for all statistical analysis. Measurement data were expressed as $\chi \pm s$. The *t*-test was used to compare the difference between the two groups. Single-factor analysis of variance (ANOVA) was used to compare the differences among groups with different concentrations. Least Significant Difference (LSD) test or Student-Newman-Keuls (SNK) test was used for pairwise comparison under the condition of homogeneity of variance. $p<0.05$ was considered statistically significant. All experiments were repeated for 3 times.

Results

MiR-34a Reduces Glial Inflammation by Inhibiting Notch Pathway

In vitro, we first used miR-34a mimics transfection and LPS activation to explore the role of miR-34a in microglial inflammatory activation. During 24 h of LPS treatment, we detected the expression of inflammation biomarkers in microglia at the protein level. Microglial inflammatory activation contributed to the overexpression of induced-nitric oxide synthase (iNOS) and CD11b, which were considered as inflammatory microglia markers. However, administration of miR-34a mimics could reverse the accumulation of inflammation. This displayed that iNOS and CD11b were significantly reduced when compared with the only LPS activated group (Figure 1A). Subsequently, we further detected the miR-34a affected signaling pathway by qRT-PCR. The results demonstrated that activated microglia significantly up-regulated the expressions of Notch1 and its ligand Jagged1. Meanwhile, activation of Notch pathway accelerated the activation of microglia and infiltration in inflammatory cells. After LPS stimulation, the expression of Notch1 and Jagged1 increased remarkably in microglia. However, administration of miR-34a mimics reversed the abnormal reduction of miR-34a in SCI tissues, which also suppressed the Notch pathway through down-regulating the expressions of Notch1 and Jagged1 (Figure 1B). Therefore, miR-34a could suppress microglia inflammation by down-regulating the Notch pathway *in vitro*.

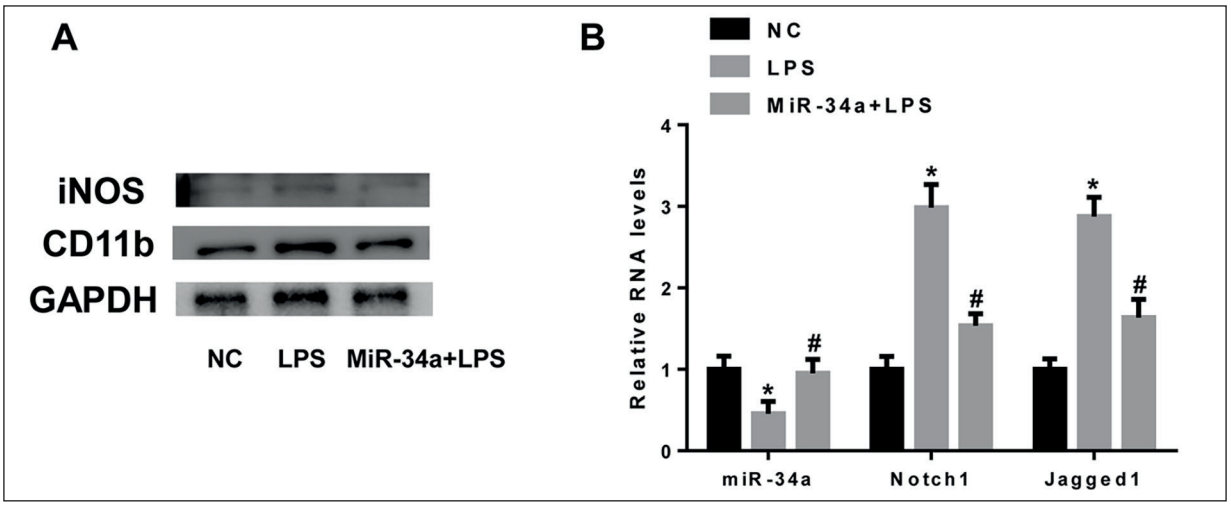

Figure 1. MiR-34a reduces glial inflammation by inhibiting Notch pathway. **A,** Protein expressions of iNOS and CD11b in NC, LPS, and miR-34a+LPS group. **B,** Changes in the mRNA expressions of miR-34a, Notch 1, and Jagged 1.

MiR-34a Inhibited Notch Pathway and Limited Inflammatory Progress Following SCI In Vivo

In SCI modeled rats, we detected the degree of miR-34a transcription and Notch pathway expression at the RNA level. Down-regulation of miR-34a at post-SCI was accompanied by the decrease of Notch pathway. However, intradural injection of miR-34a mimics rescued the SCI-induced decrease of miR-34a. Meanwhile, overexpression of Notch pathway was modified (Figure 2A). Besides, we measured the expressions of inflammatory markers, including interleukin-1 beta (IL-1β), interleukin-6 (IL-6) and monocyte chemoattractant protein-1 (MCP-1). In response to SCI, the levels of inflammatory mediators were significantly elevated at 2 days following the injury. However, excessive expression of inflammation could aggravate neural damage and negatively modulate the recovery of the injury site. MiR-34a administration effectively dominated the delivery of inflammatory mediators at 2 days post-SCI (Figure 2B). Furthermore, immunofluorescence results showed inflammatory microglia expression in the injured site. Meanwhile, a decreased number of inflammatory microglia was observed in the spinal cord of miR-34a mimics treated rats (Figure 2C). These results illustrated that miR-34a was positively regulated in the progression of glial inflammatory in the acute inflammatory phase following SCI.

Treatment of MiR-34a Modified Nervous Lesion Through Inhibiting Apoptosis

Neural renovation shows an absolute advantage in functional recovery. Ensuring the survival of damaged neurons and promoting axon regeneration in the lesion site are critical to neurological function. In this study, we measured the expression of apoptotic-related proteins to estimate the effect of miR-34a on apoptosis progression at 7 days after SCI. Poly ADP-ribose polymerase-1 (PARP-1) and Dynamin-related protein-1 (Drp-1) were detected to determine the curative effect of miR-34a treatment in anti-apoptosis. The results displayed that the decrease of PARP-1 was significantly remedied *via* injection of miR-34a

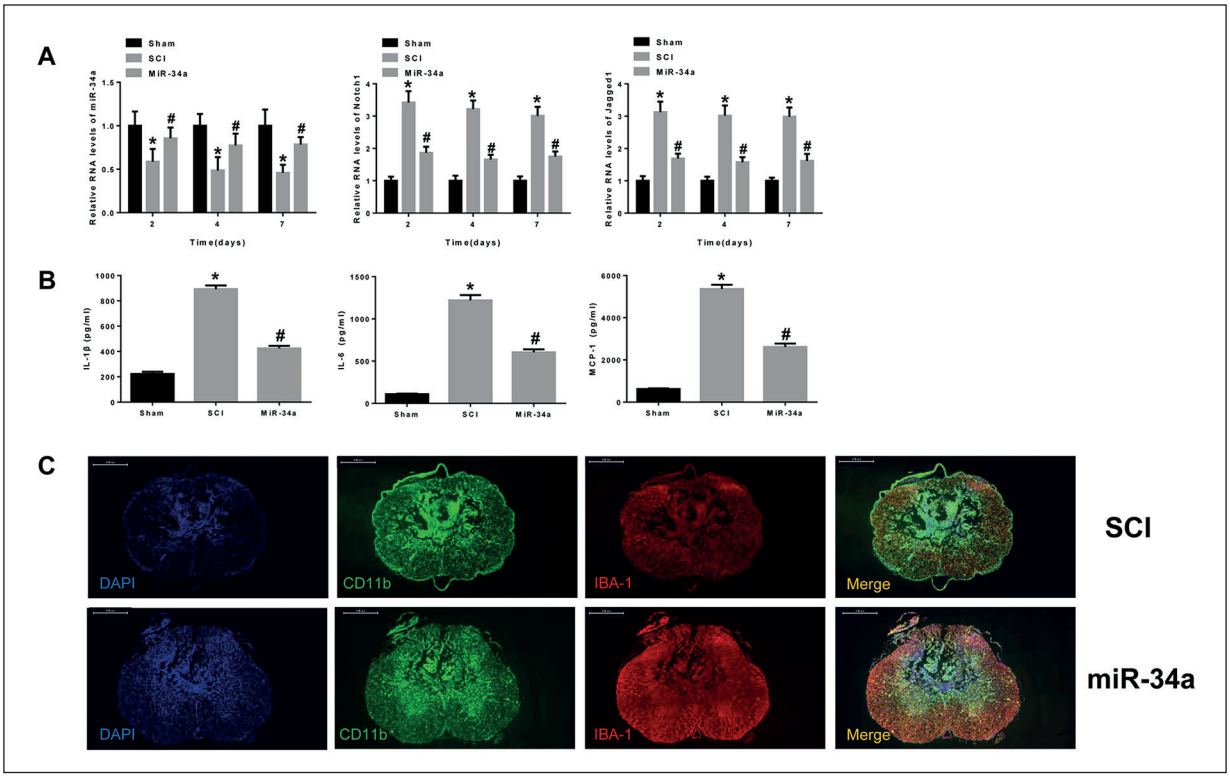

Figure 2. MiR-34a inhibited Notch pathway and limited inflammatory progress following SCI *in vivo*. **A,** RNA levels of miR-34a, Notch 1, and Jagged 1 in Sham, SCI, miR-34a group during one week after SCI. **B,** Contents of IL-1 β, IL-6, and MCP-1 in lesion at 2 days following SCI. **C,** Positive-inflammatory microglia immunofluorescence of CD11b (green) and IBA-1 (red) co-staining (magnification × 20).

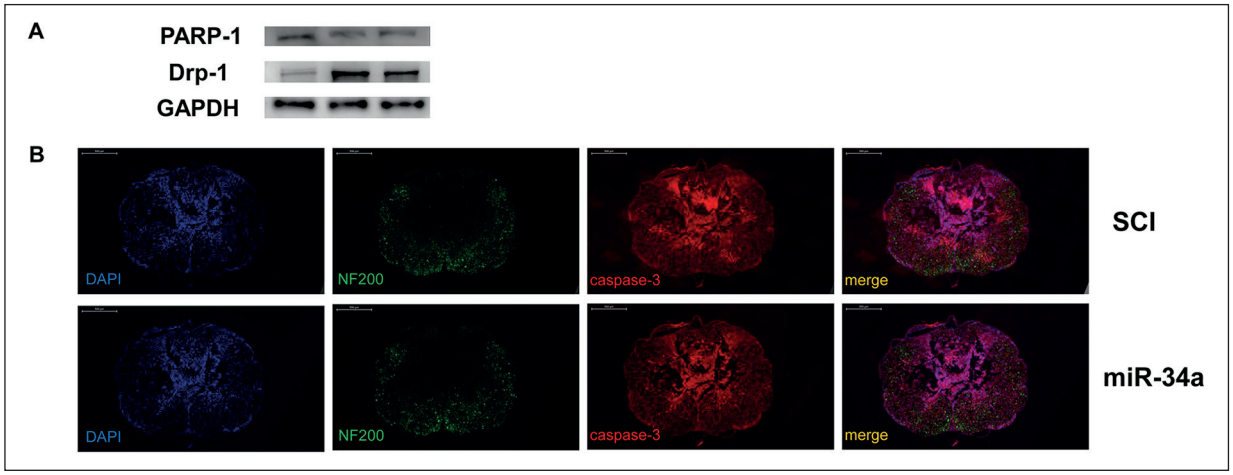

Figure 3. Treatment of miR-34a modified nervous lesion through inhibiting apoptosis. **A,** Protein expressions of PARP-1 and Drp-1 in lesion at 7 days after SCI. **B,** Apoptosis degree and neural construction immunofluorescence of NF 200 (green), and caspase-3 (red) co-staining (magnification × 20).

mimics when compared with SCI group. Inversely, the expression of Drp-1 was markedly reduced in miR-34a mimic group due to the inhibition of apoptosis. Moreover, co-staining of NF-200 and caspase-3 reflected the expression of neuro-filaments and the degree of apoptosis (Figure 3A). According to the results of immunofluorescence, the number of neuro-filaments in miR-34a mimics injected rats was remarkably higher than that of SCI rats. In addition, the caspase-3 level was remarkably down-regulated when compared with SCI group (Figure 3B). All these results indicated that the function of miR-34a contributed to the anti-apoptotic effect and neuro-structural salvage following SCI.

Locomotor Function Recovery was Mended in SCI Rats Owing to Administration of MiR-34a

All rats underwent SCI were assessed by BBB rating scale. Two blinded investigators scored the locomotor capacity of rats in an open field during four weeks at post-SCI. The results revealed that locomotor recovery of rats varied hardly and at low score at the first 3 days after injury. The therapeutic effect of miR-34a was exhibited at motor function distinction until the 7th day after SCI. Statistically significant differences were observed between SCI group and miR-34a mimic group at 28 days (Figure 4). These findings suggested that miR-34a therapy ultimately repaired SCI-induced locomotor function drawback in rats.

Discussion

The microenvironment of spinal cord tissues after SCI is critical for neurocyte survival and axon regeneration[20]. Primary injury provokes vascular changes and inflammatory stimulation in the injury site. Meanwhile, secondary damage aggravates lesion degree and area on the base of biological cascades[21,22]. Vasogenic inflammatory cells get through the disrupted vascular

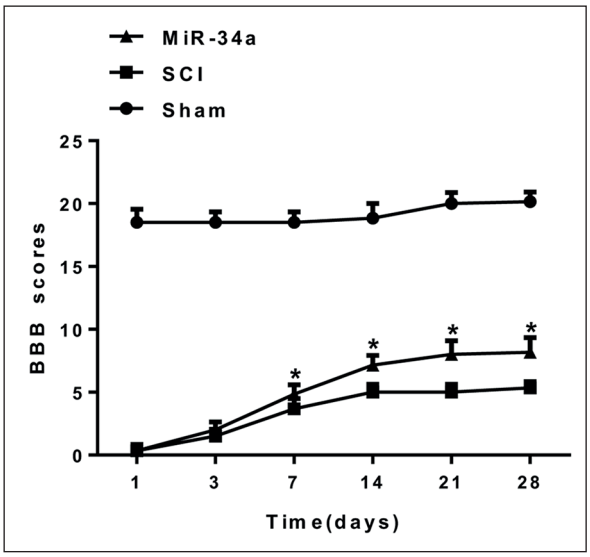

Figure 4. Locomotor function recovery was mended in SCI rat owing to administration of miR-34a. The recovery of motor function detected by BBB rating scores for 4 weeks at post-SCI.

wall to the injury site and induce inflammatory response owing to primary injury[23]. Continuous irritation of inflammation progress contributes to the activation and proliferation of microglia and hypertrophy, as well as accumulation of astrocytes[24]. Inflammation-induced formation of glial scar goes against space for axon regeneration, which inhibits molecules secreted by glial scar impede neuro-structural rehabilitation[25,26]. Besides, inflammation aggravates neuron damage and mediates the launch of cell apoptosis[27]. Current studies have demonstrated that inflammation has a profound influence on the development of SCI. Notch signaling pathway is an important signal transduction pathway that controls cell fate through interactions with adjacent cells[28,29]. In the central nervous system, both resting and activated microglia express molecules related to the Notch pathway. Meanwhile, activated microglia up-regulates the expression of Notch1 and its ligand Jagged1[30]. In addition, activation of Notch pathway may accelerate the activation of microglia and the infiltration of inflammatory cells[31]. In this study, the expression of Notch1 increased significantly after LPS stimulation in microglia. Blocking the Notch1 pathway reduced the expressions of IL-1, IL-6, iNOS, and other pro-inflammatory factors[32]. In the present report, we found that miR-34a was significantly down-regulated after SCI. Meanwhile, we verified the anti-inflammatory effect of miR-34a inhibiting notch pathway by up-regulation of miR-34a expression. In addition, miR-34a reduced the degree of apoptosis in damaged regional tissues, preserved the effective number of neurons and axons, and promoted the recovery of locomotor function. The anti-inflammatory and neuro-protective effects of miR-34a promoted the recovery of neural function after SCI. This exerted important research value in improving the regulation of the microenvironment in injury sites. This discovery also opened a new horizon for the treatment of nerve injury, and improved the mechanism and regulatory pathway of miRNA in neuro-traumatic diseases.

Conclusions

The above data showed that miR-34a suppresses neuronal apoptosis and alleviates microglia inflammation by negatively targeting the Notch pathway, thereby improving neural recovery and locomotor function.

Conflict of Interest

The Authors declare that they have no conflict of interests.

References

1) Liu Z, Ding Y, Zeng YS. A new combined therapeutic strategy of governor vessel electro-acupuncture and adult stem cell transplantation promotes the recovery of injured spinal cord. Curr Med Chem 2011; 18: 5165-5171.
2) Lin CA, Duan KY, Wang XW, Zhang ZS. MicroRNA-409 promotes recovery of spinal cord injury by regulating ZNF366. Eur Rev Med Pharmacol Sci 2018; 22: 3649-3655.
3) Hayta E, Elden H. Acute spinal cord injury: a review of pathophysiology and potential of non-steroidal anti-inflammatory drugs for pharmacological intervention. J Chem Neuroanat 2018; 87: 25-31.
4) Johnstone M, Gearing AJ, Miller KM. A central role for astrocytes in the inflammatory response to beta-amyloid; chemokines, cytokines and reactive oxygen species are produced. J Neuroimmunol 1999; 93: 182-193.
5) Ye S, Lowther S, Stambas J. Inhibition of reactive oxygen species production ameliorates inflammation induced by influenza A viruses via upregulation of SOCS1 and SOCS3. J Virol 2015; 89: 2672-2683.
6) Gwak YS, Kang J, Unabia GC, Hulsebosch CE. Spatial and temporal activation of spinal glial cells: role of gliopathy in central neuropathic pain following spinal cord injury in rats. Exp Neurol 2012; 234: 362-372.
7) Fang Y, Huang X, Wan Y, Tian H, Tian Y, Wang W, Zhu S, Xie M. Deficiency of TREK-1 potassium channel exacerbates secondary injury following spinal cord injury in mice. J Neurochem 2017; 141: 236-246.
8) Hu R, Duan B, Wang D, Yu Y, Li W, Luo H, Lu P, Lin J, Zhu G, Wan Q, Feng H. Role of acid-sensing ion channel 1a in the secondary damage of traumatic spinal cord injury. Ann Surg 2011; 254: 353-362.
9) Ogata A, Furukawa C, Sakurai K, Iba H, Kitade Y, Ueno Y. Biaryl modification of the 5'-terminus of one strand of a microRNA duplex induces strand specificity. Bioorg Med Chem Lett 2010; 20: 7299-7302.
10) Kim CW, Han JH, Wu L, Choi JY. MicroRNA-183 is essential for hair cell regeneration after neomycin injury in zebrafish. Yonsei Med J 2018; 59: 141-147.
11) Braconi C, Kogure T, Valeri N, Huang N, Nuovo G, Costinean S, Negrini M, Miotto E, Croce CM, Patel T. MicroRNA-29 can regulate expression of the long non-coding RNA gene MEG3 in hepatocellular cancer. Oncogene 2011; 30: 4750-4756.
12) Chen K, Rajewsky N. The evolution of gene regulation by transcription factors and microRNAs. Nat Rev Genet 2007; 8: 93-103.

13) Anglicheau D, Muthukumar T, Suthanthiran M. MicroRNAs: small RNAs with big effects. Transplantation 2010; 90: 105-112.

14) Liu NK, Xu XM. MicroRNA in central nervous system trauma and degenerative disorders. Physiol Genomics 2011; 43: 571-580.

15) Williams AE, Perry MM, Moschos SA, Larner-Svensson HM, Lindsay MA. Role of miRNA-146a in the regulation of the innate immune response and cancer. Biochem Soc Trans 2008; 36: 1211-1215.

16) Rivera-Barahona A, Perez B, Richard E, Desviat LR. Role of miRNAs in human disease and inborn errors of metabolism. J Inherit Metab Dis 2017; 40: 471-480.

17) Hu JZ, Huang JH, Zeng L, Wang G, Cao M, Lu HB. Anti-apoptotic effect of microRNA-21 after contusion spinal cord injury in rats. J Neurotrauma 2013; 30: 1349-1360.

18) Bhalala OG, Pan L, Sahni V, McGuire TL, Gruner K, Tourtellotte WG, Kessler JA. MicroRNA-21 regulates astrocytic response following spinal cord injury. J Neurosci 2012; 32: 17935-17947.

19) Jee MK, Jung JS, Choi JI, Jang JA, Kang KS, Im YB, Kang SK. MicroRNA 486 is a potentially novel target for the treatment of spinal cord injury. Brain 2012; 135: 1237-1252.

20) Zheng B, Lee JK, Xie F. Genetic mouse models for studying inhibitors of spinal axon regeneration. Trends Neurosci 2006; 29: 640-646.

21) Trabold R, Schueler OG, Eriskat J, Plesnila N, Baethmann AJ, Back T. Arterial hypotension triggers perifocal depolarizations and aggravates secondary damage in focal brain injury. Brain Res 2006; 1071: 237-244.

22) Skold MK, Risling M, Holmin S. Inhibition of vascular endothelial growth factor receptor 2 activity in experimental brain contusions aggravates injury outcome and leads to early increased neuronal and glial degeneration. Eur J Neurosci 2006; 23: 21-34.

23) Liu JL, Tian DS, Li ZW, Qu WS, Zhan Y, Xie MJ, Yu ZY, Wang W, Wu G. Tamoxifen alleviates irradiation-induced brain injury by attenuating microglial inflammatory response in vitro and in vivo. Brain Res 2010; 1316: 101-111.

24) Jung H, Toth PT, White FA, Miller RJ. Monocyte chemoattractant protein-1 functions as a neuromodulator in dorsal root ganglia neurons. J Neurochem 2008; 104: 254-263.

25) Rhodes KE, Moon LD, Fawcett JW. Inhibiting cell proliferation during formation of the glial scar: effects on axon regeneration in the CNS. Neuroscience 2003; 120: 41-56.

26) Rodriguez JP, Coulter M, Miotke J, Meyer RL, Takemaru K, Levine JM. Abrogation of beta-catenin signaling in oligodendrocyte precursor cells reduces glial scarring and promotes axon regeneration after CNS injury. J Neurosci 2014; 34: 10285-10297.

27) Vincenzi F, Ravani A, Pasquini S, Merighi S, Gessi S, Setti S, Cadossi R, Borea PA, Varani K. Pulsed electromagnetic field exposure reduces hypoxia and inflammation damage in neuron-like and microglial cells. J Cell Physiol 2017; 232: 1200-1208.

28) Sirakov M, Boussouar A, Kress E, Frau C, Lone IN, Nadjar J, Angelov D, Plateroti M. The thyroid hormone nuclear receptor TRalpha1 controls the Notch signaling pathway and cell fate in murine intestine. Development 2015; 142: 2764-2774.

29) Liu L, Wada H, Matsubara N, Hozumi K, Itoh M. Identification of domains for efficient notch signaling activity in immobilized notch ligand proteins. J Cell Biochem 2017; 118: 785-796.

30) Yuan Y, Rangarajan P, Kan EM, Wu Y, Wu C, Ling EA. Scutellarin regulates the Notch pathway and affects the migration and morphological transformation of activated microglia in experimentally induced cerebral ischemia in rats and in activated BV-2 microglia. J Neuroinflammation 2015; 12: 11.

31) Grandbarbe L, Michelucci A, Heurtaux T, Hemmer K, Morga E, Heuschling P. Notch signaling modulates the activation of microglial cells. Glia 2007; 55: 1519-1530.

32) Cao Q, Lu J, Kaur C, Sivakumar V, Li F, Cheah PS, Dheen ST, Ling EA. Expression of Notch-1 receptor and its ligands Jagged-1 and Delta-1 in amoeboid microglia in postnatal rat brain and murine BV-2 cells. Glia 2008; 56: 1224-1237.